$HClO_4$ in MeCN at 298 K can also be calculated by using eq 9-11. In contrast with electron-transfer reactions involving ferrocene derivatives, the observed values in Table III are 10^9-fold larger than the calculated values, as shown in Figure 6. The huge enhancement of the observed rates relative to the calculated ones may be attributed to a strong inner-sphere character in the acid-catalyzed electron transfer from CoTPP to dioxygen. Such a strong inner-sphere nature suggests that the electron transfer gives a complex, $CoTPPO_2H^{\bullet+}$, in which a strong interaction between $CoTPP^+$ and $HO_2^\bullet$ causes a significant reduction of Gibbs energy change of electron transfer from CoTPP to dioxygen in the presence of $HClO_4$ (eq 13). The further reduction of $HO_2^\bullet$

$$CoTPP + O_2 + H^+ \rightarrow CoTPPO_2H^{\bullet+} \quad (13)$$

to H_2O_2 by CoTPP in the presence of $HClO_4$ may proceed via $CoTPPO_2H^{\bullet+}$ (eq 14), since the oxidizing ability of $HO_2^\bullet$ is

$$CoTPPO_2H^{\bullet+} + CoTPP + H^+ \rightarrow 2CoTPP^+ + H_2O_2 \quad (14)$$

increased by the ligand to metal charge-transfer (LMCT) interaction with $CoTPP^+$. Thus, the combination of an outer-sphere electron transfer from Fc to $CoTPP^+$ with an inner-sphere electron transfer from CoTPP to O_2 in the presence of $HClO_4$ constitutes an efficient catalytic cycle, as shown in Scheme I.

The same type of interaction in $Co(TIM)O_2H^{\bullet3+}$ as in $CoTPPO_2H^{\bullet+}$ may reduce the energy barrier for electron transfer from ferrocene derivatives to $Co(TIM)^{3+}$ in the presence of $HClO_4$ and dioxygen in MeCN. The rate constants of electron transfer from ferrocene derivatives to $Co(TIM)^{3+}$ cannot be obtained directly, since the electron transfer is not only reversible but also endothermic. However, the rate constants can be estimated by the calculation based on eq 9-11 from the values of the one-electron oxidation potential of $Co(TIM)^{3+}$ (-0.12 V vs SCE) and the reported value of the self-exchange rate constant (6.0×10^{-2} M^{-1} s^{-1}),[40] together with the corresponding values for ferrocene derivatives noted above. In Figure 7, the observed rate constants log k_{obs} of electron transfer from various ferrocene derivatives to $Co(TIM)^{3+}$ in the presence of O_2 (1.3×10^{-2} M) and $HClO_4$ (1.0×10^{-2} M) are plotted against the oxidation potentials of ferrocene derivatives ($E_{ox}°$). On the other hand, the calculated dependence of log k_{12} on $E_{ox}°$ is shown by the dotted line. The observed rate constants of various ferrocene derivatives are larger than the calculated ones by about the same magnitude irrespective of ferrocene derivatives, indicating the inner-sphere nature of the electron transfer. At present, however, the exact mechanism of the inner-sphere electron transfer is not known.

(40) Durham, B.; Endicott, J. F.; Wong, C.-L.; Rillema, D. P. *J. Am. Chem. Soc.* **1979**, *101*, 847.

Contribution from the Service de Chimie Organique, Université Libre de Bruxelles, B.P. 160, 50 avenue Franklin Roosevelt, 1050 Bruxelles, Belgium, and Department of Chemistry, Katholieke Universiteit Leuven, B-3030 Leuven, Belgium

Resonance Raman Spectra and Spectroelectrochemical Properties of Mono- and Polymetallic Ruthenium Complexes with 1,4,5,8,9,12-Hexaazatriphenylene

A. Kirsch-De Mesmaeker,*,†,‡ L. Jacquet,† A. Masschelein,†,§ F. Vanhecke,‖ and K. Heremans‖

Received December 6, 1988

The resonance Raman spectra of the monometallic heteroleptic complexes of HAT (1,4,5,8,9,12-hexaazatriphenylene) and bpy (2,2′-bipyridine) are discussed as a function of the excitation wavelength, in relation to the MLCT (metal to ligand charge transfer) transitions from the Ru^{2+} to the ligand HAT or bpy and to the spectroelectrochemical correlation obtained from the spectroscopic and electrochemical data. The same analyses are performed with the bi- and trimetallic complexes $[Ru(bpy)_2^{2+}]_2HAT$ and $[Ru(bpy)_2^{2+}]_3HAT$, respectively. In the trimetallic compound, the large and intense MLCT band centered around 580 nm is attributed only to Ru-HAT transitions and the much less intense band, at ~400 nm, to Ru-bpy transitions. SERR (surface enhanced resonance Raman) spectra, recorded when rR measurements were not possible because of some luminescence of the complexes, emphasize specific effects of the silver sol.

Introduction

We have explored previously[1] the possibilities of 1,4,5,8,9,12-hexaazatriphenylene (HAT) as a ligand for transition metals, especially ruthenium. Thus, the trishomoleptic $Ru(HAT)_3^{2+}$ (I) and the heteroleptic complexes with 2,2′-bipyridine (bpy) $Ru(HAT)_n(bpy)_{3-n}^{2+}$ (n = 1, 2) were successfully obtained and characterized. The main interest, however, in the HAT ligand stems from its ability to behave as a unique symmetric bridging ligand for polymetallic complexes. Indeed, one can either complex up to three $Ru(bpy)_2^{2+}$ moieties around one central HAT and thus prepare the mono-, bi-, and trimetallic complexes, $[Ru(bpy)_2^{2+}]_n(HAT)$ (n = 1-3; II, n = 3), or one can also start from $Ru(HAT)_3^{2+}$ (I) and chelate two $Ru(L)_2^{2+}$ species (L = ligand) on each HAT to obtain up to seven Ru^{2+} ions in the same molecule.

These HAT complexes present many interesting properties: for instance, $Ru(bpy)_2(HAT)^{2+}$ behaves as a very good DNA intercalator;[2] it is also, as the bimetallic $[Ru(bpy)_2^{2+}]_2(HAT)$ species, an attractive synthetic precursor for heterometallic edifices where intramolecular electron and energy transfer could be studied. Moreover, for some derivatives of these polymetallic complexes, their direct electropolymerization or incorporation into a polymer

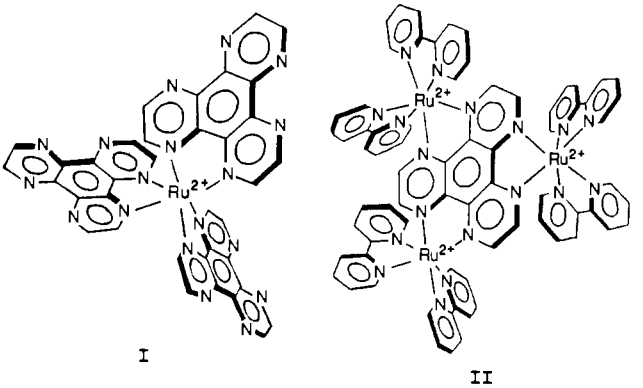

I II

* To whom correspondence should be addressed.
† Université Libre de Bruxelles.
‡ Senior Research Associate of the National Fund for Scientific Research (Belgium).
§ Research Assistant of the National Fund for Scientific Research (Belgium).
‖ Katholieke Universiteit Leuven.

(1) Masschelein, A.; Kirsch-De Mesmaeker, A.; Verhoeven, C.; Nasielski-Hinkens, R. *Inorg. Chim. Acta* **1987**, *129*, L13-16.
(2) Kelly, J.; Tossi, A.; Kirsch-De Mesmaeker, A.; Masschelein, A. To be submitted for publication.

0020-1669/89/1328-2465$01.50/0

on an electrode can also be considered in view of their electrocatalytic properties.

All those potential applications require a full and complete understanding of the photophysical properties of these HAT complexes; in particular their spectroscopic study by resonance Raman (rR) spectroscopy, which is the focus of this paper, can provide much interesting information.

Since approximately 1981, the literature documents well the rR spectra of Ru complexes in the ground and in the electronically excited state.[3-9] For instance, for some monometallic[10-12] and bimetallic[13-15] heteroleptic complexes, studies of excitation profiles in rR spectra allowed the assignment of different Ru–ligand transitions as a function of the wavelength within the MLCT (metal to ligand charge transfer) absorption band, showing the localized character of the electron transition to a specific ligand. In parallel to these studies, the spectroelectrochemical correlation obtained with many different ligands[16,17] during these last few years also gave rise to a finer characterization of the MLCT absorption bands.

Interestingly, and more directly related to the work presented here, a study on a bimetallic complex with 4′,7′-phenanthrolino-5′,6′:5,6-pyrazine,[15] similar to the bimetallic HAT complex except for the absence of the extra nitrogen atoms, emphasized, by comparison with the dimer formed with 2,3-bis(2-pyridyl)pyrazine,[13,14] that the excitation profile in rR spectra depends strongly on the nature of the bridging ligand.

In the present study, we focus our interest on the dependence of the resonance Raman spectra on the excitation wavelength, for the monometallic $Ru(HAT)_n(bpy)_{3-n}^{2+}$ (n = 1–3) and polymetallic $[Ru(bpy)_2^{2+}]_nHAT$ (n = 2, 3) complexes; this is correlated with their MLCT absorption characteristics, depending on the number of chelated Ru^{2+} ions, and with their spectroelectrochemical properties. The aim is to examine how the electronic Ru–bpy and Ru–HAT transitions shift in energy in these different complexes, especially in the trimetallic molecule.

Since it is generally difficult to obtain rR spectra at excitation wavelengths corresponding to the red portion of the MLCT absorption, because of important background noise due to the luminescence of the complexes, we recorded also the spectra in the presence of a silver sol, which efficiently quenches the luminescence and which is known to enhance rR spectra by surface interactions (SERR effect); this is discussed in detail elsewhere.[18a]

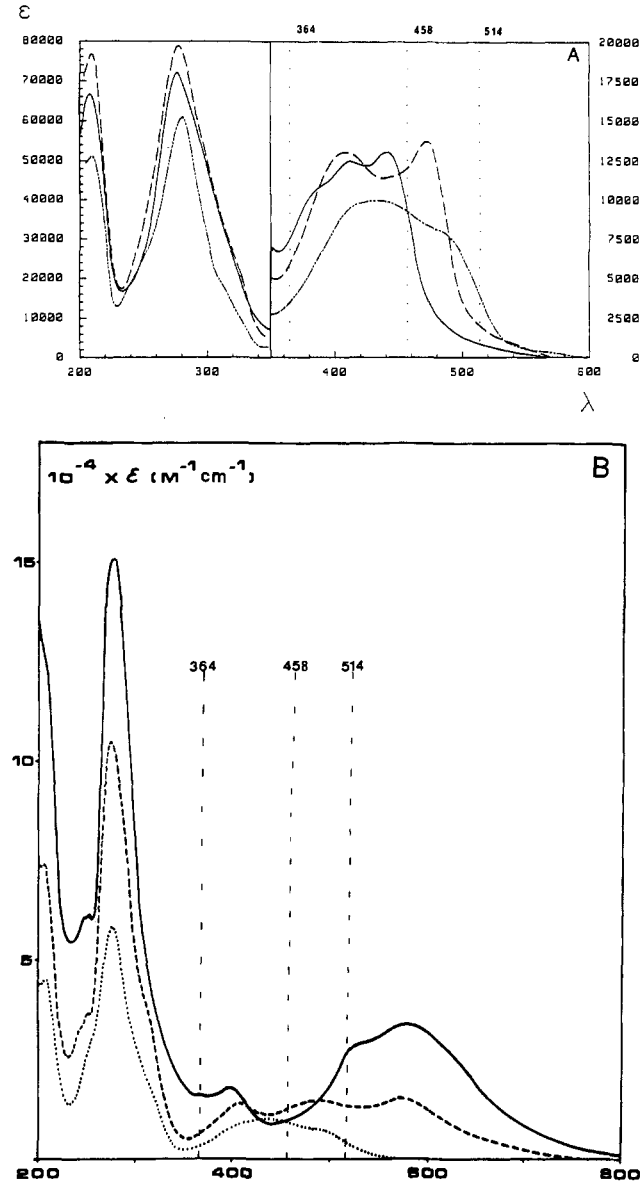

Figure 1. Absorption spectra of HAT complexes in water: (A) monometallic complexes $Ru(bpy)_2HAT^{2+}$ (–··–), $Ru(bpy)(HAT)_2^{2+}$ (––), and $Ru(HAT)_3^{2+}$ (—); (B) $Ru(bpy)_2(HAT)^{2+}$ (···), $[Ru(bpy)_2]_2HAT^{4+}$ (– – –), and $[Ru(bpy)_2]_3HAT^{6+}$ (—).

Experimental Section

The preparation and characterization of $Ru(HAT)(bpy)_2^{2+}$, $[Ru(bpy)_2^{2+}]_2HAT$, and $[Ru(bpy)_2^{2+}]_3HAT$ have been described previously.[1]

$Ru(HAT)_3^{2+}$ was synthesized and purified as follows. An aqueous solution of $Ru(DMSO)_4Cl_2$ was refluxed under argon in presence of an excess of HAT; the occurrence of $Ru(HAT)_2X_2$ (X = Cl^-, H_2O) and its transformation into $Ru(HAT)_3^{2+}$ were detected by absorption spectrophotometry and by TLC on silica gel (95:5 $HCCl_3$:MeOH) and on a Whatman SiC18 reverse phase (1:1 CH_3CN:MeOH, 0.015 M CH_3SO_3H). The complex was obtained in 70% yield after purification on a cation exchanger (Sephadex SP C25, elution with 0.5 M NaCl) and precipitation with KPF_6.

$Ru(bpy)(HAT)_2^{2+}$ was prepared by refluxing, under argon, an aqueous solution of $Ru(bpy)Cl_4^{2-}$ obtained as described in the literature[21] in the presence of an excess of HAT. The complexes have been characterized by their NMR spectra (Bruker, 250 MHz); their UV and visible absorption spectra were recorded with a Varian Cary 219 spectrophotometer.

It has to be noted that, although each monometallic complex belongs to a specific point group, this is not the case for the bi- and trimetallic complexes. Indeed, two diastereomers belonging to different point groups

(3) Carrol, P. J.; Brus, L. E. *J. Am. Chem. Soc.* **1987**, *109*, 7613–7616.
(4) Kumar, Ch. V.; Barton, J. K.; Turro, N. J.; Gould, I. R. *Inorg. Chem.* **1987**, *26*, 1455–1457.
(5) Balk, R. W.; Stufkens, D. J.; Crutchley, R. J.; Lever, A. B. P. *Inorg. Chim. Acta* **1982**, *64*, L49–50.
(6) Mabrouk, P. A.; Wrighton, M. S. *Inorg. Chem.* **1986**, *25*, 526–531.
(7) Chung, Y. C.; Leventis, N.; Wagner, P. J.; Leroi, G. E. *Inorg. Chem.* **1985**, *24*, 1966–1968.
(8) Casper, J. V.; Westmoreland, T. D.; Allen, G. H.; Bradley, P. G.; Meyer, T. J.; Woodruff, W. H. *J. Am. Chem. Soc.* **1984**, *106*, 3492–3500.
(9) Bradley, P. J.; Kress, N.; Hornberger, B. A.; Dallinger, R. F.; Woodruff, W. H. *J. Am. Chem. Soc.* **1981**, *103*, 7441.
(10) McClanahan, S. F.; Dallinger, R. F.; Holler, F. J. Kincaid, J. R. *J. Am. Chem. Soc.* **1985**, *107*, 4853–4860.
(11) Chung, Y. C.; Leventis, N.; Wagner, P. J.; Leroi, G. E. *J. Am. Chem. Soc.* **1985**, *107*, 1414–1416.
(12) Chung, Y. C.; Leventis, N.; Wagner, P. J.; Leroi, G. E. *J. Am. Chem. Soc.* **1985**, *107*, 1416–1417.
(13) Knorrs, C.; Gafney, H. D.; Baker, A. D.; Braunstein, C. Strekas, T. C. *J. Raman Spectrosc.* **1983**, *14*, 32–35.
(14) Braunstein, C. H.; Baker, A. D.; Strekas, T. C.; Gafney, H. D. *Inorg. Chem.* **1984**, *23*, 857–864.
(15) Fuchs, Y.; Lofters, S.; Dieter, T.; Shi, W.; Morgan, R.; Strekas, T. C.; Gafney, H. D.; Baker, A. D. *J. Am. Chem. Soc.* **1987**, *109*, 2691–2697.
(16) Barigelletti, F.; Juris, A.; Balzani, V.; Belser, P.; von Zelewsky, A. *Inorg. Chem.* **1987**, *26*, 4115–4119.
(17) Ohsawa, Y.; Hanck, K. W.; DeArmond, M. K. *J. Electroanal. Chem. Interfacial Electrochem.* **1984**, *175*, 229.
(18) (a) Vanhecke, F.; Heremans, K.; Kirsch-De Mesmaeker, A.; Jacquet, L.; Masschelein, A. Submitted for publication in *J. Raman Spectrosc.* (b) Hildebrand, P.; Stockburger, M. *J. Phys. Chem.* **1986**, *90*, 6017.
(19) (a) Kirsch-DeMesmaeker, A.; Nasielski-Hinkens, R.; Maetens, D.; Pauwels, D.; Nasielski, J. *Inorg. Chem.* **1984**, *23*, 377–379. (b) To be submitted for publication.
(20) Balzani, V.; Juris, A.; Barrigelletti, F.; Belser, P.; von Zelewsky, A. *Sci. Pap. Inst. Phys. Chem. Res. (Jpn.)* **1984**, *78*, 78.
(21) Krause, R. A. *Inorg. Chim. Acta* **1979**, *22*, 209–213.

Table I[a]

$Ru(bpy)_3^{2+}$ rR	HAT R	$Ru(HAT)_3^{2+}$ rR	$Ru(HAT)_3^{2+}$ SERR	$Ru(HAT)_2(bpy)^{2+}$ rR	$Ru(HAT)(bpy)_2^{2+}$ rR
			1028		
1034*					1036*
	1042				
			1063		1064
		1120	1119		
1180*					1182*
			1188		
		1238	1240	1235	1236
1280*					1282*
	1307	1309	1307	1307	1307
1322*					1322*
	1338		1346		
	1397	1393	1388	1389	1398
	1409				
		1435	1430	1434	1430
	1478				
1494*		1495	1493	1492**	1496**
					1534
	1517				
	1545	1542	1540	1541	
1566*					1566*
	1581				
		1601	1601	1604	1602
1610*					

[a] Vibration frequencies in cm^{-1} corresponding to the rR and SERR spectra at 458 nm for the complexes in aqueous solutions. For free HAT, the Raman spectrum is given at 514 nm in $CHCl_3$ (second column). A single asterisk means assignment to bpy, and two asterisks denote overlapping of the bpy and HAT bands. Underlined values correspond to HAT vibration frequencies common to free HAT and the complexes.

can be found in each polynuclear complex: Λ^2 (and its enantiomer Δ^2, C_2 group) and $\Lambda\Delta$ (C_s group) for $[Ru(bpy)_2^{2+}]_2(HAT)$; Δ^3 (and its enantiomer Λ^3, D_3 group) and $\Lambda\Delta^2$ (and its enantiomer $\Delta\Lambda^2$, C_2 group) for $[Ru(bpy)_2^{2+}]_3(HAT)$. Since these diastereoisomers have not been separated,[1] the rR spectra discussed in this paper correspond to their mixtures.

Aqueous colloidal silver was prepared according to the citrate reduction method.[18b] Scattered light was registered with either a Spex 1403 double monochromator with photon-counting detection or with a Spex Triplemate equipped with an OMA III system. Excitation was with an Ar^+ Spectra-Physics 2020 laser system with selection of the 364-, 458-, and 514-nm laser lines. Wavelength calibration was done with indene. The spectral slit width was 7 cm^{-1}. Resonance spectra were taken at millimolar concentrations with 200-mW power at the laser head. SERRS spectra were taken at concentrations on the order of 10^{-7} M with 300-mW power at the laser head; the wavenumbers are given within ±2 cm^{-1}.

Redox potentials were determined by cyclic voltammetry on a homemade platinum-disk electrode (approximate area ~20 mm^2) in acetonitrile. The potential of the working electrode was controlled by a homemade potentiostat versus a saturated calomel electrode (Radiometer K701) separated from the solution by a Tacussel bridge; the counter electrode was a large-area platinum grid.

The supporting electrolyte was in all cases tetrabutylammonium hexafluorophosphate (Fluka puriss.). Acetonitrile (Aldrich Gold Label) was carefully distilled from P_2O_5 and stored over molecular sieves. The solutions were deoxygenated by bubbling dry nitrogen for at least 20 min.

Results

1. Absorption Spectra. Parts A and B of Figure 1 give the absorption spectra, respectively, of the monometallic complexes $Ru(HAT)_3^{2+}$, $Ru(HAT)_2(bpy)^{2+}$, and $Ru(HAT)(bpy)_2^{2+}$ and of the bi- and trimetallic compounds $[Ru(bpy)_2^{2+}]_2HAT$ and $[Ru(bpy)_2^{2+}]_3HAT$. The MLCT bands present several peaks, the most intense one being at the longer wavelength, except for $Ru(HAT)(bpy)_2^{2+}$; the three excitation wavelengths within the MLCT band are also shown.

2. Resonance Raman Spectra of Monometallic HAT Complexes. Excitation at 458 nm. Parts A and B of Figure 2 show the rR spectra from 1000 to 1650 cm^{-1}, obtained by excitation at 458 nm, of the two HAT heteroleptic monometallic complexes; Table I gives the corresponding vibration frequencies as well as those of the trishomoleptic complexes $Ru(bpy)_3^{2+}$ and $Ru(HAT)_3^{2+}$, also at 458 nm for comparison. The rR spectrum of $Ru(HAT)_3^{2+}$ (not shown) presents an important background noise due to luminescence; this noise can be suppressed by adding a silver sol,[18] increasing tremendously the vibration intensities (SERR effect). We therefore also give in Table I the corresponding values for the SERR spectrum of $Ru(HAT)_3^{2+}$. The frequencies of the Raman spectrum of the free ligand HAT (at 514 nm) are also included for comparison. The asterisks indicate the characteristic vibrations of bpy and the double asterisks an overlapping between a bpy and a HAT vibration. The vibrational bands in the rR spectra of the HAT heteroleptic complexes that do not correspond to bpy vibrations have been attributed to the HAT ligand by comparison with the frequencies of the rR and SERR spectra of $Ru(HAT)_3^{2+}$.

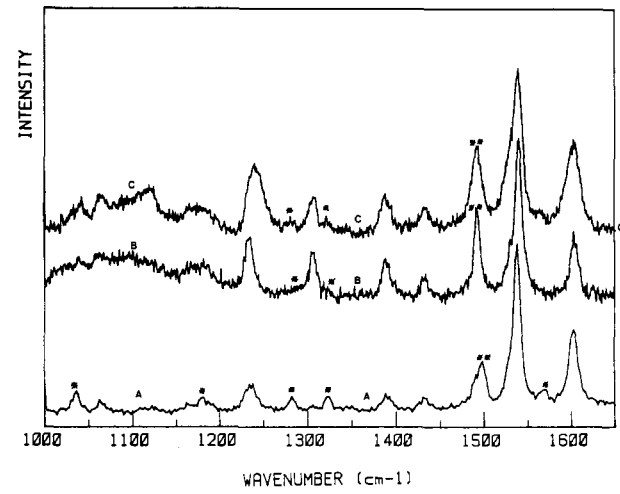

Figure 2. Spectra at 458 nm for aqueous solutions: (A) rR spectrum of 1 mM $Ru(bpy)_2(HAT)^{2+}$; (B) rR spectrum of 1 mM $Ru(bpy)(HAT)_2^{2+}$; (C) SERR spectrum of 10^{-3} mM $Ru(bpy)(HAT)_2^{2+}$. A single asterisk denotes bpy vibrations; two asterisks denote overlapping of bpy and HAT vibrations.

It can be observed from Table I that there are only two or three Raman frequency vibrations of free HAT (underlined) that are common to the rR spectra of the complexes. The 1234–1240-cm^{-1} vibration corresponds to the pyrazine-like vibration,[15] which is resonance-enhanced and therefore is not detected in the Raman spectrum of free HAT.

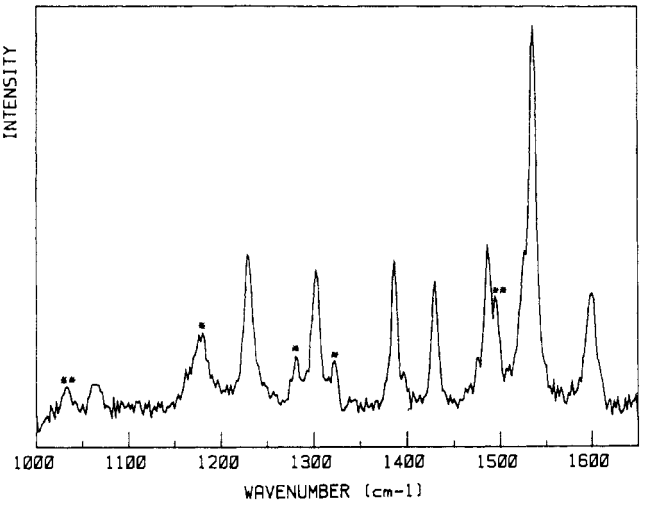

Figure 3. rR spectrum at 514 nm of 1 mM $Ru(bpy)_2(HAT)^{2+}$ in water (cf. Figure 2 for an explanation of asterisks).

For $Ru(HAT)_3^{2+}$ and $Ru(HAT)_2(bpy)^{2+}$, the 458-nm excitation falls into the most bathochromic peak of the MLCT band, but for $Ru(HAT)(bpy)_2^{2+}$, this wavelength falls between the most bathochromic and the most intense peak in the MLCT band.

In Figure 2A, for $Ru(HAT)(bpy)_2^{2+}$, the vibration characteristics of the bpy ligand are easily detected; in contrast, in Figure 2B, for $Ru(HAT)_2(bpy)^{2+}$, they are scarcely visible and a HAT vibration at 1307 cm^{-1} has appeared. Figure 2C shows the SERR spectrum of $Ru(HAT)_2(bpy)^{2+}$ also at 458 nm; it is similar to its rR spectrum (Figure 2B; a detailed study of the SERR effect is given elsewhere[18a]).

Comparison between Excitations at 458 nm and 514 nm. The comparison of the spectra at 458 and 514 nm, where the latter wavelength corresponds to the tail of the absorption of $Ru(HAT)_2(bpy)^{2+}$ and is closer to the λ_{max} value of the most bathochromic peak in the MLCT band of $Ru(HAT)(bpy)_2^{2+}$, leads to the following observations. For $Ru(HAT)(bpy)_2^{2+}$ (Figure 3 at 514 nm, Figure 2A at 458 nm), one can notice that, from 458 to 514 nm, several vibrations attributed to HAT have increased in intensity as compared to the intensities of the bpy vibrations (compare, for instance, the relative intensities at 1280*, 1302, and 1322* cm^{-1}, in Figures 2A and 3).

It was not possible to record a rR spectrum of $Ru(HAT)_2(bpy)^{2+}$ at 514 nm, again because of the background noise due to its luminescence; with the silver sol, however, a SERR spectrum (not shown) was obtained and is similar to the rR spectrum at 458 nm (Figure 2B) with slight differences in the intensities of the HAT vibrations. Since, when comparison is possible between a rR and a SERR spectrum at the same excitation wavelength (Figure 2B,C at 458 nm), no silver influence can be detected, by extrapolation, one should turn to the SERR spectrum of $Ru(HAT)_2(bpy)^{2+}$ at 514 nm for comparison with its rR spectrum at 458 nm. Thus as already mentioned, both of these spectra at those two wavelengths are similar and the bpy vibrations at 1280* and 1322* cm^{-1} are masked by the important HAT peak at 1302 cm^{-1}.

Excitation at 364 nm. RR spectra have also been recorded with excitation at 364 nm (not shown), corresponding to an absorption between the MLCT and $\pi-\pi^*$ bands; in that case bpy and HAT vibrations are identified in $Ru(HAT)_2(bpy)^{2+}$, whereas only bpy vibrations are detected in $Ru(bpy)_2(HAT)^{2+}$. The assignments of the bpy and HAT frequencies have been made by comparison with the rR spectra of the two trishomoleptic complexes $Ru(bpy)_3^{2+}$ and $Ru(HAT)_3^{2+}$ at 364 nm.

In order to summarize the influence of the excitation wavelength described here, Table II gives the different contributions of the ligands in the spectra recorded at the three wavelengths (364, 458, 514 nm). Thus, for $Ru(HAT)_2(bpy)^{2+}$, bpy vibrations are clearly detected only at 364 nm whereas almost exclusively HAT vibrations are present at the two other wavelengths; for $Ru(bpy)_2(HAT)^{2+}$, the relative contribution of the bpy vibrations decreases as compared to that of the HAT vibrations, as one goes to longer excitation wavelengths.

Table II. Relative Contribution of the Ligands in Four Complexes at Different Excitation Wavelengths[a]

complex	364 nm rR	458 nm rR	458 nm SERR	514 nm rR	514 nm SERR
$Ru(HAT)_2(bpy)^{2+}$	b + H	~H			~H
$Ru(bpy)_2(HAT)^{2+}$	b	H + (b)		H↑ + (b)	
$[Ru(bpy)_2]_2HAT^{4+}$	b	H + (b)	b	H	H + b
$[Ru(bpy)_2]_3HAT^{6+}$	b	H + (b)	b	H	b

[a] Legend: H, HAT; b, bpy; (b), small contribution of bpy; H↑, increased contribution of HAT.

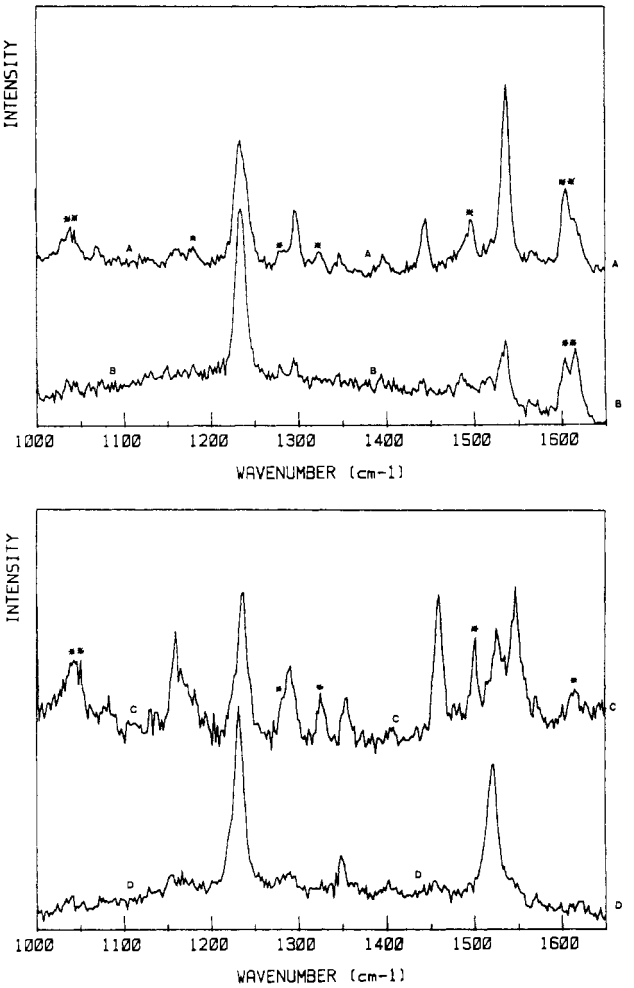

Figure 4. rR spectra of the polymetallic complexes 1 mM in water: (A) bimetallic complex at 458 nm; (B) bimetallic complex at 514 nm; (C) trimetallic complex at 458 nm; (D) trimetallic complex at 514 nm (cf. Figure 2 for an explanation of asterisks).

3. Resonance Raman Spectra of the Bi- and Trimetallic Complexes. The rR spectrum of the bimetallic complex at 458 nm, i.e. with excitation between the first and second peak composing the visible absorption band (from the blue to the red, Figure 1B), is shown in Figure 4A: the most intense vibrations are characteristic of HAT; however, bpy vibrations can also be detected. On excitation at 514 nm, thus between the second and the third peak of the visible absorption band, the bpy vibrations have almost vanished and the most intense HAT vibration appears now at 1234 cm^{-1} instead of 1534 cm^{-1}, corresponding thus to the resonance-enhanced pyrazine-like vibration (Figure 4B).

Parts C and D of Figure 4 show the rR spectra of the trimetallic complex illuminated at 458 and 514 nm. The 458-nm excitation, between the large band centered around 580 nm and the less intense one at ~400 nm, gives rise to bpy and HAT vibrations, whereas on excitation at 514 nm, only three HAT vibrations are visible in the rR spectrum, at 1522 and 1348 cm^{-1} and the most

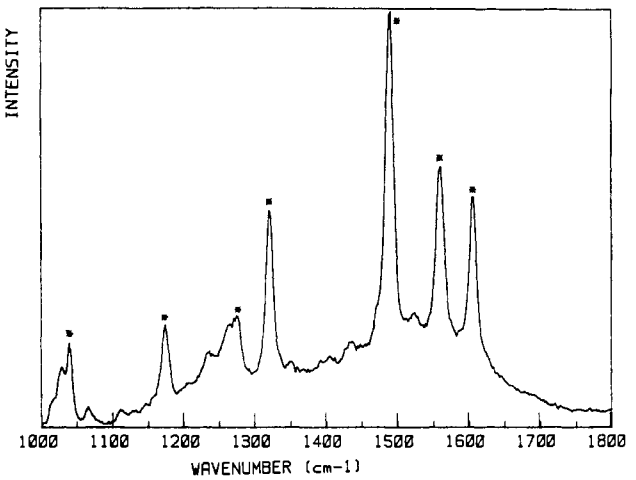

Figure 5. SERR spectrum of 10^{-3} mM trimetallic complex at 514 nm (cf. Figure 2 for an explanation of asterisks).

intense at 1232 cm^{-1}, as in the bimetallic complex. One could wonder why, in the rR spectra of the polymetallic derivatives, many characteristic vibration frequencies of the HAT ligand are missing compared to the monometallic spectra. This originates probably from the important enhancement of the pyrazine-like vibration (1234 cm^{-1}) in the polymetallic compounds as compared to the other vibrations and could be correlated with the fact that in the polymetallic derivatives both nitrogen atoms of a pyrazine-like ring form a σ bond with a Ru^{2+} ion, inducing some changes in the polarizability of bonds involved in the vibrations.

The main observations for the bi- and trimetallic complexes are also summarized in Table II, where we see, moreover, that at 364 nm only the bpy vibrations are detectable for both complexes.

It was not possible to record the rR spectra by excitation at 600 nm, again because of the luminescence of the compounds; we therefore recorded their SERR spectra at that wavelength. The effects of the silver sol that we then observed prompted us to perform a new investigation of SERR spectra not only of the polymetallic complexes but also of the monometallic HAT complexes under 600-nm excitation, although those compounds do not absorb at that wavelength in the absence of silver colloid; this study is given elsewhere.[18a] We comment here only on the SERR spectra of the bi- and trimetallic complexes under excitation wavelengths examined in this paper, i.e. 458 and 514 nm, in order to emphasize that the wavelength influence on the rR spectra developed here can be in some cases completely different in the presence of a silver sol. Thus, for the bimetallic compound at 514 nm, bpy vibrations are clearly observable, and at 458 nm almost exclusively bpy frequencies are detected. For the trimetallic complex, at 514 (Figure 5) and 458 nm only the characteristic vibrations of bpy are observed.

A comparison of these results with those obtained by rR spectroscopy thus without silver sols, shows obviously that the bpy contribution increases in SERR spectra. This is clearly summarized in Table II, where we see that for the polymetallic complexes, at 458 nm, vibrations from HAT and, in lower proportion, from bpy are observed by rR spectroscopy, whereas by SERR spectroscopy, only bpy is detected; at 514 nm, only HAT characteristics are visible by rR spectroscopy whereas by SERR spectroscopy bpy frequencies are also observed and are the only ones present in the trimetallic compound.

4. Spectroelectrochemical Correlation. In order to know whether the HOMO–LUMO transitions of the mono- and polymetallic HAT complexes originate from the same orbitals as the redox orbitals involved in their first oxidation and reduction waves, we tried to correlate their absorption energies with the redox potential data.

Table III gives the potentials of the first oxidation and reduction waves of the five complexes, their differences ($\Delta E_{1/2}$), the λ_{max} value of the most bathochromic peak in the MLCT band, and its

Table III[a]

complexes	no.	E_{ox}^1, V vs SCE	E_{red}^1, V vs SCE	$\Delta E_{1/2}$, V	λ_{max}, nm	λ_{max}, eV
$Ru(HAT)_3^{2+}$	5	+2.07	−0.62	2.69	440	2.806
$Ru(HAT)_2(bpy)^{2+}$	4	+1.79	−0.76	2.55	472	2.616
$Ru(HAT)(bpy)_2^{2+}$	3	+1.56	−0.84	2.40	484	2.551
$[Ru(bpy)_2^{2+}]_2(HAT)$	2	+1.53	−0.49	2.02	572	2.158
$[Ru(bpy)_2^{2+}]_3(HAT)$	1	+1.61	−0.25	1.86	580	2.128

[a] Redox potentials of the first oxidation and reduction of five HAT complexes, determined by cyclic voltammetry on a glassy-carbon electrode (in acetonitrile with 0.1 M Bu_4NPF_6), their differences ($\Delta E_{1/2}$), and the λ_{max} values of the most bathochromic peak of the MLCT band. The numbering of the complexes corresponds to that in Figure 6.

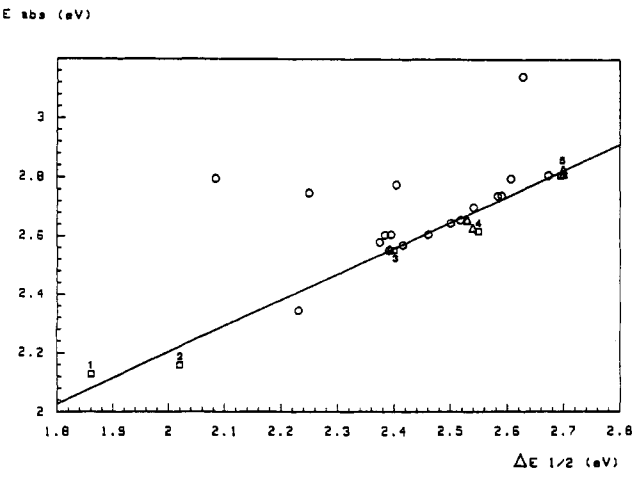

Figure 6. Plot of the transition energy of absorption versus $\Delta E_{1/2}$ for the five complexes of Table III (□; for the numbering, see the corresponding complex in Table III), for complexes with HAT, 1,4,5,8-tetraazaphenanthrene, and bpy prepared in our laboratory (△),[19] and for some analogues whose data were taken from the literature (○).[17,20]

corresponding energy in electronvolts. The reduction potentials of the first reduction wave can be attributed to a HAT reduction in all the cases because the values are not negative enough for a bpy reduction.[1] It can be seen that the more HAT ligands a complex contains, the more positive is its oxidation potential, due to a stabilization of the $d\pi$ orbitals by back-bonding to the HAT ligand. In contrast, these $d\pi$ orbitals do not seem to be stabilized from the mono- to the bi- to the trimetallic complex since the first oxidation potentials remain more or less constant; the most important difference occurs between the bi- and the trinuclear compounds (only ~80 mV).

In Figure 6, we plotted the transition energy of absorption versus $\Delta E_{1/2}$, for the five complexes and for some complexes in the literature. It can be seen that the spectroelectrochemical correlation for the HAT complexes is rather good, in agreement with the fact that the λ_{max} energy of the most bathochromic peak in the visible absorption band corresponds to an electronic transition from a $d\pi$ metallic orbital (oxidation redox orbital) to a π^* antibonding orbital of the HAT ligand (reduction redox orbital), thus to a charge transfer from the metal to the most oxidizing ligand.

Discussion

The spectroelectrochemical correlation is in agreement with the rR spectra since, with an excitation wavelength corresponding to or approaching the most bathochromic peak of absorption, the spectra show almost exclusively the vibration frequencies of HAT.

Moreover, from these rR results, it is also possible to draw some conclusions on the electronic transitions composing the visible absorption bands of the mono- and polymetallic compounds, which we discuss hereafter in more detail by referring to the spectra of Figure 1 and to the summary of the rR data in Table II.

1. Bisheteroleptic Monometallic Complexes. For the two monometallic heteroleptic complexes, the rR results and the spectroelectrochemical correlation indicate clearly that the most

bathochromic peak of the MLCT band corresponds mainly to a Ru–HAT transition.

Indeed for $Ru(HAT)_2bpy^{2+}$, the rR and SERR spectra show that at 514 nm (in the tail of the most bathochromic peak composing the MLCT band), and at 458 nm (between the two peaks, closer to the most bathochromic peak maximum), almost exclusively HAT frequencies are observed. For $Ru(HAT)(bpy)_2^{2+}$, probably composed of three transitions (484 and 434 nm and a shoulder at 410 nm), the most bathochromic peak leads to the spectroelectrochemical correlation; this indicates also that it should be attributed to a Ru–HAT transition. In agreement with this, at 514 nm the rR spectrum shows an increased contribution of vibrations from the HAT ligand as compared to an excitation at 458 nm, which is closer to the λ_{max} value of the second absorption maximum and where the bpy vibrations are clearly present. To be complete, the study for both heteroleptic complexes should also present data for an excitation at 400 nm, where mainly the bpy frequencies should be detected, but this wavelength is not available.

If we examine the results for an excitation at 364 nm, thus in the blue region of the MLCT band, one observes the following. For $Ru(HAT)_2(bpy)^{2+}$, the rR spectrum indicates the presence of bpy and also of HAT frequencies (these latter frequencies could however originate from some HAT π–π^* transitions and not only from MLCT transitions). For $Ru(HAT)(bpy)_2^{2+}$, the bpy signals are the only ones detected at 364 nm.

Consequently, from the results in the blue and in the red portion of the MLCT band of the heteroleptic complexes, it is clear that some overlap of the MLCT transition to HAT with the MLCT transition to bpy is present; this looks reasonable, if we take into account the fact that for a "metal to a specific ligand charge transfer" there are probably transitions to states of different symmetry, as in $Ru(HAT)_3^{2+}$, where the MLCT band is composed of three peaks. This mixture of MLCT transitions, observed at some wavelengths, can also be rationalized on the basis of the visible absorption spectra and of the oxidation potentials of the complexes.

Figure 1A shows that the whole MLCT band shifts hypsochromically from $Ru(HAT)(bpy)_2^{2+}$ to $Ru(HAT)_2(bpy)^{2+}$ to $Ru(HAT)_3^{2+}$, thus when the number of bpy decreases, meaning that not only the Ru–HAT but also the Ru–bpy transition(s) is blue-shifted; both of them are indeed influenced similarly by the ancillary ligands. The dπ orbital participating in a transition, toward a HAT or a bpy ligand, is more stabilized when more HAT ancillary ligands are present, due to the better π-acceptor properties of HAT as compared to those of bpy. This is evidenced by comparing the oxidation potentials of the monometallic complexes in Table III, which become more positive, from $Ru(HAT)(bpy)_2^{2+}$ to $Ru(HAT)_2(bpy)^{2+}$ to $Ru(HAT)_3^{2+}$. Taking into account these considerations, one understands easily why, at 364 nm, HAT signals are still present in $Ru(HAT)_2(bpy)^{2+}$ and not in $Ru(HAT)(bpy)_2^{2+}$ and why, at 514 nm, bpy signals are still observable in $Ru(HAT)(bpy)_2^{2+}$ and not in $Ru(HAT)_2(bpy)^{2+}$.

2. Bi- and Trimetallic Complexes. By comparing the visible absorption spectra of figure 1B, we are tempted to conclude that as we go from the mono- to the bi- to the trimetallic complex, the Ru–bpy transitions are more and more separated from the Ru–HAT transitions within the MLCT bands, so that, in the trimetallic compound, the Ru–HAT transitions would seem to be centered around 580 nm and the Ru–bpy ones around 400 nm. This could be checked by rR spectroscopy, as mentioned in the Introduction.

Despite the fact that data for an excitation around 400 nm are missing, some conclusions can nevertheless be drawn concerning that question.

With the bimetallic compound (Table II), it is indeed possible that the first peak centered around 410 nm would correspond mainly to Ru–bpy transitions since, at 364 nm, only bpy vibrations are observable and, at 458 nm, at the beginning of the second band, bpy frequencies can still be detected and become of the same order of magnitude as the background noise at 514 nm, past the maximum of the second component of the visible absorption band.

The case of the trimetallic complex (Table II) is rather clear since, at 458 nm, between the first band at ~390 nm and the second very intense one at 580 nm, bpy vibrations are observed in the rR spectrum and vanish with an excitation at 514 nm, the rR spectrum showing then only a few HAT vibrations; moreover, since at 580 nm the transition can be correlated with the electrochemical data, meaning that it should also correspond to a Ru–HAT transition, we can safely conclude that the whole visible band from 514 nm to the red can be attributed to Ru–HAT transitions. The fact that the first band maximizing at ~390 nm, thus originating from Ru–bpy transitions, seems to be blue shifted compared to the bands for the other complexes could be attributed to a slight stabilization of the dπ orbital (the first oxidation potential is slightly more positive in the trimetallic compound) and maybe to some different splitting of the π^* bpy orbitals due to changes of the molecular symmetry. Although the intensity of the band at 390 nm could correspond to that of an MLCT transition, some contribution of a MC (metal-centered) transition may not be excluded in this wavelength region.

Another striking feature emerging from Figure 1B is that, although the intensity of the π–π^* transition around 280 nm increases proportionally with the number of $Ru(bpy)_2^{2+}$ moieties, this is not obvious for the Ru–HAT transitions in the MLCT band. In fact it is unreasonable to discuss the relative intensity of the Ru–HAT chromophore in the three complexes because this chromophore is probably strongly affected by the change of symmetry in these molecules, generating a different splitting of the orbitals and thus other sets of allowed and forbidden transitions.

In the case of a monometallic complex, it is clear that the presence of a silver sol does not invert the relative contribution of the bpy and HAT ligands in the SERR spectrum as compared to the rR spectrum (compare part C of Figure 2 with part B), whereas with the bi- and trimetallic complexes, the silver sol makes the contribution of the bpy much more important (Table II; compare Figure 4D with Figure 5). Actually, this spectacular enhancement of the bpy signals in the SERR spectra of the polymetallic complexes, as compared to the intensity of the HAT signals in the rR spectra, could be explained by steric arguments. If we refer to the trimetallic compound (II), one can conclude that a contact between HAT and the silver surface of the sol is probably not possible because the central ligand is shielded by the $Ru(bpy)_2^{2+}$ moieties, so that only the bpy frequencies are surface-enhanced. In the case of the bimetallic compound, some shielding of the HAT ligand from the silver sol could still be present, whereas in the monometallic complex, HAT becomes as accessible as bpy to the silver particles.

Acknowledgment. We thank Professor J. Nasielski for his helpful discussions. L.J. wishes to thank the "Institut pour l'Encouragement de la recherche scientifique dans l'industrie et l'agriculture" (IRSIA), and F.V. the "Institut voor Wetenschappelijk Onderzoek in Nijverheid en Landbouw (IWONL), for a fellowship.